

Irreducible Three-Loop Vacuum-Polarization Correction in Muonic Bound Systems

Gregory S. Adkins¹ and Ulrich D. Jentschura²

¹*Department of Physics and Astronomy, Franklin & Marshall College, Lancaster, Pennsylvania, 17604, USA*

²*Department of Physics and LAMOR, Missouri University of Science and Technology, Rolla, Missouri 65409, USA*

Three-loop electronic vacuum-polarization corrections due to irreducible diagrams are evaluated for two-body muonic ions with nuclear charge numbers $1 \leq Z \leq 6$. The corrections are of order $\alpha^3(Z\alpha)^2 m_r$, where α is the fine-structure constant and m_r is the reduced mass. Numerically, the energy corrections are found to be of the same order-of-magnitude as the largest of the order $\alpha^2(Z\alpha)^6 m_r$ corrections, and are thus phenomenologically interesting. Our method of calculation eliminates numerical uncertainty encountered in other approaches.

I. INTRODUCTION

Energy corrections to bound states of muonic ions due to electronic vacuum-polarization effects are known to be numerically large, due to the smallness of the generalized Bohr radius of the muonic ions. For the n -loop energy shift $E^{(n)}$, one obtains the estimates $E^{(n)} \sim \alpha^n (Z\alpha)^2 m_r$, where α is the fine-structure constant, Z is the nuclear charge number, and m_r is the reduced mass of the two-body system.

In particular, the two-loop vacuum-polarization contributions to the $2P-2S$ energy shift in muonic hydrogen has recently been re-evaluated in Ref. [1]. From the irreducible two-loop diagrams, one obtains a contribution of 1.25298 meV [see Eq. (71) of Ref. [1]], while, from the reducible diagram, one obtains 0.25495 meV [see Eq. (72) of Ref. [1]]. These results confirm the two-loop corrections obtained in Ref. [2]. The sum of the two-loop contributions is about five times larger than the energy shift corresponding to the so-called proton radius puzzle [3–5].

Hence, it is of interest to consider the three-loop vacuum polarization effect for the bound states in muonic ions. The scalar vacuum polarization function $\Pi^{(3)}(q^2)$ describing the irreducible three-loop vacuum-polarization diagrams has been discussed in its asymptotic (short-distance, high q^2) limit in the context of the Gell-Mann Low ψ function (see Ref. [6]) and for the Callan-Symanzik renormalization group (see Ref. [7]). The evaluation of three-loop vacuum-polarization corrections in bound systems relies on knowledge of $\Pi^{(3)}(q^2)$ beyond the asymptotic (short-distance) regime. The three-loop vacuum polarization spectral density function $\text{Im}[\Pi_{\text{R}}^{(3)}(q^2)]$ has recently been evaluated analytically [8]. Using the spectral density, the full three-loop vacuum polarization function $\Pi_{\text{R}}^{(3)}(q^2)$ can be conveniently obtained using a subtracted dispersion relation.

For muonic bound states, the evaluation of three-loop energy corrections has been discussed in Refs. [9–11]. Here, we are concerned with the evaluation of the irreducible three-loop contribution, which, from the point of view of quantum field theory, probably constitutes the conceptually most interesting, gauge-invariant, subset of three-loop corrections.

This paper is organized as follows. Some relevant properties of the spectral function of three-loop vacuum-

polarization function are discussed in Sec. II, before we consider the numerical evaluation of the three-loop energy shifts in Sec. III. Conclusions are reserved for Sec. IV. We use natural units in this paper with $\hbar = c = \epsilon_0 = 1$. In addition, we use the “West-Coast” convention for the space-time metric: $g_{\mu\nu} = \text{diag}(1, -1, -1, -1)$, where $\mu, \nu = 0, 1, 2, 3$.

II. ANALYTIC DERIVATION

Our calculations make extensive use of the spectral function of three-loop vacuum polarization, which was recently obtained expressed in terms of generalized polylogarithms in Ref. [8]. The irreducible three-loop diagrams are shown in Fig. 1. We use the vacuum-polarization function in the conventions of Ref. [1] and assume it to be renormalized on-shell so that $\Pi_{\text{R}}(0) = 0$. We consider the expansion

$$\Pi_{\text{R}}(q^2) = \Pi_{\text{R}}^{(1)}(q^2) + \Pi_{\text{R}}^{(2)}(q^2) + \Pi_{\text{R}}^{(3)}(q^2) + \dots, \quad (1)$$

where the superscript denotes the loop order. Each order separately fulfills the subtracted dispersion relation

$$\Pi_{\text{R}}^{(n)}(q^2) = \frac{q^2}{\pi} \int_{4m_e^2}^{\infty} dq'^2 \frac{\text{Im}[\Pi_{\text{R}}^{(n)}(q'^2 + i\epsilon)]}{q'^2(q'^2 - q^2)}. \quad (2)$$

where care has been taken to fulfill the condition that $\Pi_{\text{R}}^{(n)}(q^2)$ needs to vanish for zero q^2 . We scale the n th loop order as in Eq. (11a) of Ref. [1],

$$\Pi_{\text{R}}^{(n)}(q^2) = \left(\frac{\alpha}{\pi}\right)^n P_{\text{R}}^{(n)}(q^2). \quad (3)$$

When comparing to Eq. (2.1) and Eq. (3.9) of Ref. [8], one realizes that the relation of our n th-loop function $\Pi_{\text{R}}^{(n)}$ and the $\rho^{(n)}$ of Ref. [8] is

$$\text{Im}[\Pi_{\text{R}}^{(n)}(q^2)] = \left(\frac{\alpha}{4\pi}\right)^n \rho^{(n)}(q^2). \quad (4)$$

which implies, in particular, that

$$\text{Im}[P_{\text{R}}^{(n)}(q^2)] = \frac{\rho^{(n)}(q^2)}{2^{2n}}. \quad (5)$$

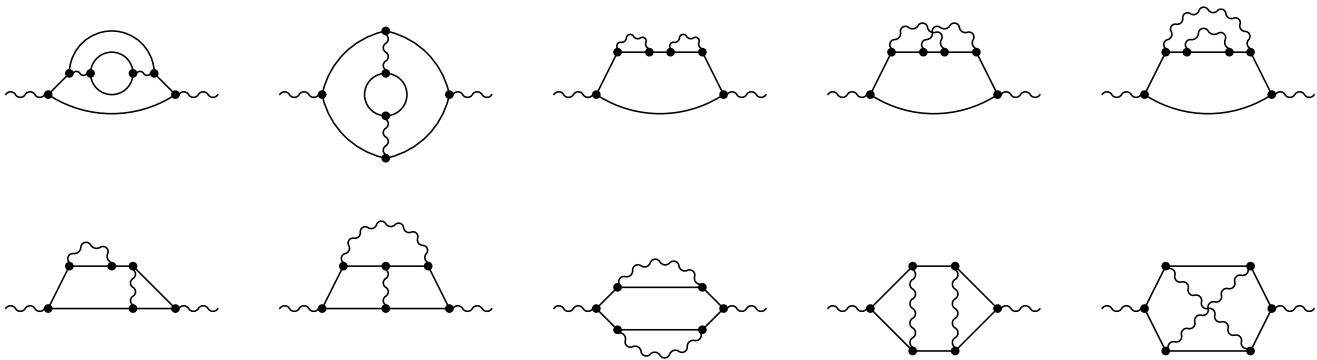


FIG. 1. The irreducible three-loop vacuum-polarization diagrams are shown, with the fermion lines denoting the virtual electrons and virtual positrons.

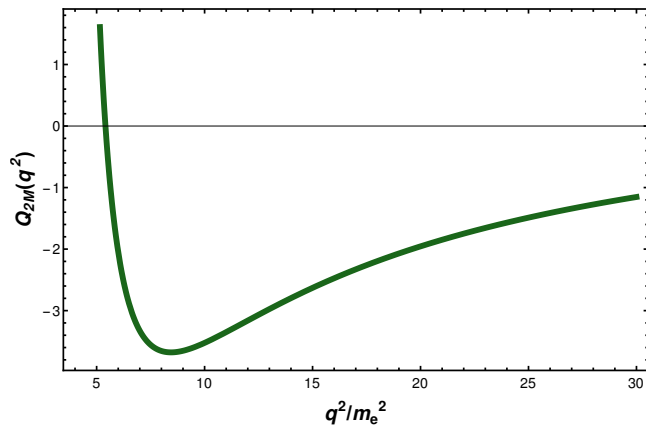


FIG. 2. The two-fermion threshold contribution to the imaginary part of the three-loop vacuum-polarization function is given as $Q_{2m}(q^2)$ in Eq. (8). It has an integrable singularity at the threshold $q^2 = (2m_e)^2$ [see Eq. (9)].

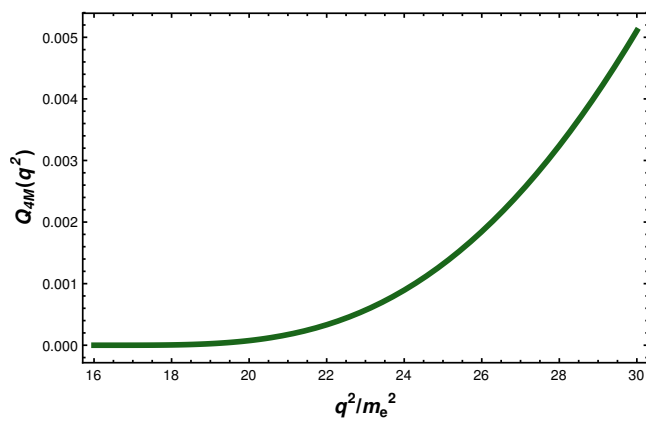


FIG. 3. Same as Fig. 2, but for the four-fermion threshold contribution $Q_{4m}(q^2)$. It ramps up smoothly from the threshold at $q^2 = (4m_e)^2$ [see Eq. (11)].

The one-loop function $\text{Im}[P_R^{(n)}(q^2)]$ is given as

$$\text{Im}[P_R^{(1)}(q^2)] = \frac{\pi}{6} v (3 - v^2) \Theta(q^2 - 4m_e^2). \quad (6)$$

This result is well known and confirmed in Eq. (28) of Ref. [1] and Eq. (3.1) of Ref. [8], upon setting the number of fermion flavors $N = 1$ in the latter and realizing that the β variable, in the notation of Ref. [8], is equal to the Schwinger v parameter [12], which reads as

$$v = \sqrt{1 - \frac{4m_e^2}{q^2}}. \quad (7)$$

The three-loop diagrams ($n = 3$) are depicted in Fig. 1. These are naturally divided into five categories. The first two diagrams in the upper row of Fig. 1 are vacuum-polarization insertions in the inner virtual photon of the two-loop effect (first category). The next category (the rightmost three diagrams in the upper row) are two-loop self-energy insertions in one of the fermion lines of the one-loop effect. The first two diagrams in the second row are self-energy and vertex corrections to the one-loop vertex correction diagram (fourth category). The last three diagrams in the lower row are generated from the one-loop vacuum-polarization graph via the insertion of an equal number of photon vertices in the upper and lower fermion lines (fifth category).

The imaginary part of the three-loop diagrams given in Fig. 1 can be written as

$$\text{Im}[P_R^{(3)}(q^2 + i\epsilon)] = Q_{2m}(q^2) \Theta(q^2 - (2m_e)^2) + Q_{4m}(q^2) \Theta(q^2 - (4m_e)^2). \quad (8)$$

where the function $Q_{2m}(q^2)$ summarizes the terms with a two-fermion threshold, where the terms with a four-fermion threshold are summarized in $Q_{4m}(q^2)$. The former are obtained, for example, by cutting the third diagram in the upper row of Fig. 1 right in the middle of the inner fermion lines, and using the Cutkosky rules [13]. However, there are additional terms with a four-fermion

TABLE I. Three-loop energy shifts due to irreducible three-loop diagrams are given for muonic bound systems in the range $1 \leq Z \leq 6$ of nuclear charge numbers, given in units of meV. The numerical uncertainties are ± 1 in the least significant digit shown.

Bound System	n	nS	nP	nD	nF
μH	$n = 1$	-2.5148×10^{-2}	—	—	—
	$n = 2$	-2.6243×10^{-3}	-6.5673×10^{-4}	—	—
	$n = 3$	-7.5797×10^{-4}	-2.0310×10^{-4}	-1.0841×10^{-5}	—
	$n = 4$	-3.1704×10^{-4}	-8.6759×10^{-5}	-6.0104×10^{-6}	-1.1495×10^{-7}
μD	$n = 1$	-2.7476×10^{-2}	—	—	—
	$n = 2$	-2.8541×10^{-3}	-7.7875×10^{-4}	—	—
	$n = 3$	-8.2386×10^{-4}	-2.3863×10^{-4}	-1.4109×10^{-5}	—
	$n = 4$	-3.4454×10^{-4}	-1.0167×10^{-4}	-7.7703×10^{-6}	-1.6478×10^{-7}
$\mu^3\text{He}$	$n = 1$	-1.6343×10^{-1}	—	—	—
	$n = 2$	-1.8071×10^{-2}	-1.2009×10^{-2}	—	—
	$n = 3$	-5.0874×10^{-3}	-3.1380×10^{-3}	-7.0445×10^{-4}	—
	$n = 4$	-2.1163×10^{-3}	-1.2868×10^{-3}	-3.3621×10^{-4}	-2.8701×10^{-5}
$\mu^4\text{He}$	$n = 1$	-1.6550×10^{-1}	—	—	—
	$n = 2$	-1.8348×10^{-2}	-1.2280×10^{-2}	—	—
	$n = 3$	-5.1618×10^{-3}	-3.2020×10^{-3}	-7.3004×10^{-4}	—
	$n = 4$	-2.1470×10^{-3}	-1.3124×10^{-3}	-3.4757×10^{-4}	-3.0182×10^{-5}
$\mu^6\text{Li}$	$n = 1$	-4.3559×10^{-1}	—	—	—
	$n = 2$	-5.6686×10^{-2}	-4.7059×10^{-2}	—	—
	$n = 3$	-1.5350×10^{-2}	-1.1362×10^{-2}	-4.9511×10^{-3}	—
	$n = 4$	-6.3292×10^{-3}	-4.5635×10^{-3}	-2.0785×10^{-3}	-3.8702×10^{-4}
$\mu^7\text{Li}$	$n = 1$	-4.3712×10^{-1}	—	—	—
	$n = 2$	-5.6952×10^{-2}	-4.7315×10^{-2}	—	—
	$n = 3$	-1.5418×10^{-2}	-1.1421×10^{-2}	-4.9946×10^{-3}	—
	$n = 4$	-6.3569×10^{-3}	-4.5864×10^{-3}	-2.0950×10^{-3}	-3.9191×10^{-4}
$\mu^9\text{Be}$	$n = 1$	-8.5559×10^{-1}	—	—	—
	$n = 2$	-1.2644×10^{-1}	-1.1033×10^{-1}	—	—
	$n = 3$	-3.3769×10^{-2}	-2.6421×10^{-2}	-1.6351×10^{-2}	—
	$n = 4$	-1.3764×10^{-2}	-1.0410×10^{-2}	-6.2674×10^{-3}	-1.9036×10^{-3}
$\mu^{10}\text{Be}$	$n = 1$	-8.5699×10^{-1}	—	—	—
	$n = 2$	-1.2672×10^{-1}	-1.1057×10^{-1}	—	—
	$n = 3$	-3.3842×10^{-2}	-2.6482×10^{-2}	-1.6410×10^{-2}	—
	$n = 4$	-1.3793×10^{-2}	-1.0433×10^{-2}	-6.2875×10^{-3}	-1.9134×10^{-3}
$\mu^{10}\text{B}$	$n = 1$	-1.4392×10^0	—	—	—
	$n = 2$	-2.3119×10^{-1}	-2.0220×10^{-1}	—	—
	$n = 3$	-6.2396×10^{-2}	-4.9895×10^{-2}	-3.7513×10^{-2}	—
	$n = 4$	-2.5110×10^{-2}	-1.9292×10^{-2}	-1.3586×10^{-2}	-5.7294×10^{-3}
$\mu^{11}\text{B}$	$n = 1$	-1.4411×10^0	—	—	—
	$n = 2$	-2.3158×10^{-1}	-2.0253×10^{-1}	—	—
	$n = 3$	-6.2507×10^{-2}	-4.9987×10^{-2}	-3.7610×10^{-2}	—
	$n = 4$	-2.5153×10^{-2}	-1.9326×10^{-2}	-1.3619×10^{-2}	-5.7509×10^{-3}
$\mu^{12}\text{C}$	$n = 1$	-2.2111×10^0	—	—	—
	$n = 2$	-3.7447×10^{-1}	-3.2349×10^{-1}	—	—
	$n = 3$	-1.0354×10^{-1}	-8.3630×10^{-2}	-7.0401×10^{-2}	—
	$n = 4$	-4.1215×10^{-2}	-3.1862×10^{-2}	-2.4732×10^{-2}	-1.3145×10^{-2}
$\mu^{13}\text{C}$	$n = 1$	-2.2132×10^0	—	—	—
	$n = 2$	-3.7490×10^{-1}	-3.2384×10^{-1}	—	—
	$n = 3$	-1.0368×10^{-1}	-8.3739×10^{-2}	-7.0519×10^{-2}	—
	$n = 4$	-4.1266×10^{-2}	-3.1902×10^{-2}	-2.4772×10^{-2}	-1.3177×10^{-2}

threshold; these are generated, for example, when one cuts the first Feynman diagram in the upper row of Fig. 1 right in the middle.

The conversion to the conventions of Ref. [8] is achieved by identifying $Q_{2m}(q^2) = \frac{1}{64} \rho_{2m}^{(3)}(q^2)$ and $Q_{4m}(q^2) = \frac{1}{64} \rho_{4m}^{(3)}(q^2)$. For reference, we list the asymptotic behavior of these functions at their respective thresholds $q^2 = (2m_e)^2$ and $q^2 = (4m_e)^2$, and for large q^2 . The threshold expansion for $Q_{2m}(q^2)$ is most easily expressed

in terms of the variable v , which is defined in Eq. (7),

$$\begin{aligned}
Q_{2m}(q^2) = & \frac{\pi^5}{24v} - \pi^3 - \frac{\pi^3 v}{3} \ln(v) + v \left[-\frac{\pi \zeta(3)}{2} \right. \\
& \left. + \frac{5\pi^5}{72} - \frac{43\pi^3}{36} + \frac{527\pi}{72} + \frac{2\pi^3}{3} \ln(2) \right] + \mathcal{O}(v^2 \ln(v)).
\end{aligned} \tag{9}$$

where we take note of the fact that $v = 0$ at the threshold $q^2 = (2m_e)^2$. Alternatively, the first terms read as follows, when expressed in terms of $q^2/m_e^2 - 4$, which also goes to zero at threshold, $Q_{2m}(q^2) = \frac{\pi^5}{12\sqrt{q^2/m_e^2 - 4}} -$

$\pi^3 + \mathcal{O}(\sqrt{q^2/m_e^2 - 4})$. The asymptotics for high q^2 of $Q_{2m}(q^2)$ involve triple logarithms,

$$Q_{2m}(q^2) = -\frac{\pi}{54} \ln^3\left(\frac{q^2}{m_e^2}\right) + \frac{19\pi}{108} \ln^2\left(\frac{q^2}{m_e^2}\right) + \left(-\frac{881\pi}{648} + \frac{13\pi^3}{108} - \frac{\pi}{3}\zeta(3)\right) \ln\left(\frac{q^2}{m_e^2}\right) - \frac{\pi}{3}\zeta(3) + \frac{19\pi^5}{1080} - \frac{\pi^3}{3}\ln(2) - \frac{89\pi^3}{216} + \frac{15767\pi}{2592} + \mathcal{O}\left(\frac{m_e^2}{q^2} \ln\left(\frac{q^2}{m_e^2}\right)\right). \quad (10)$$

The four-fermion-threshold term $Q_{4m}(q^2)$ ramps up smoothly from its threshold, without an (integrable) singularity,

$$Q_{4m}(q^2) = \frac{11\pi^2}{330301440} \left(\frac{q^2}{m_e^2} - 16\right)^{9/2} - \frac{89\pi^2}{11626610688} \left(\frac{q^2}{m_e^2} - 16\right)^{11/2} + \frac{1055\pi^2}{906875633664} \left(\frac{q^2}{m_e^2} - 16\right)^{13/2} + \mathcal{O}\left(\left(\frac{q^2}{m_e^2} - 16\right)^{15/2}\right). \quad (11)$$

The asymptotics of $Q_{4m}(q^2)$ for high q^2 cancel the double and triple logarithms from Eq. (10),

$$Q_{4m}(q^2) = \frac{\pi}{54} \ln^3\left(\frac{q^2}{m_e^2}\right) - \frac{19\pi}{108} \ln^2\left(\frac{q^2}{m_e^2}\right) + \left(\frac{935\pi}{648} - \frac{13\pi^3}{108} + \frac{\pi}{3}\zeta(3)\right) \ln\left(\frac{q^2}{m_e^2}\right) + \frac{2\pi}{3}\zeta(3) - \frac{19\pi^5}{1080} + \frac{\pi^3}{3}\ln(2) + \frac{89\pi^3}{216} - \frac{4259\pi}{648} + \mathcal{O}\left(\frac{m_e^2}{q^2} \ln\left(\frac{q^2}{m_e^2}\right)\right). \quad (12)$$

For large q^2 , in view of a considerable cancelation between $Q_{2m}(q^2)$ and $Q_{4m}(q^2)$, there is only a single logarithm left,

$$\text{Im}[P_R^{(3)}(q^2)] = Q_{2m}(q^2) + Q_{4m}(q^2) = \frac{\pi}{12} \ln\left(\frac{q^2}{m_e^2}\right) + \frac{\pi}{3}\zeta(3) - \frac{47\pi}{96} + \mathcal{O}\left(\frac{m_e^2}{q^2} \ln\left(\frac{q^2}{m_e^2}\right)\right). \quad (13)$$

From Eq. (13), with the help of the dispersion relation (2), one may infer the leading logarithmic asymptotics of $P_R^{(3)}(-\bar{q}^2)$ for large spatial momentum transfer $q^2 = -\bar{q}^2$, and compare with Ref. [14]. However, for

the non-logarithmic term, the calculation is more complicated. The non-logarithmic term for the entire three-loop function is known, and can be inferred from equations presented in the text following Eq. (4) of Ref. [15] (for the non-logarithmic term proportional to N^2) and from Eq. (15) of Ref. [16] and Eq. (4) of Ref. [17] (for the non-logarithmic term proportional to N). (Note that the quantity N , the number of fermion flavors, counts the number of electron loops in Fig. 1.) One may infer the result

$$P_R^{(3)}(-\bar{q}^2) = -\frac{1}{24} \ln^2\left(\frac{\bar{q}^2}{m_e^2}\right) + \left(\frac{47}{96} - \frac{\zeta(3)}{3}\right) \ln\left(\frac{\bar{q}^2}{m_e^2}\right) - \frac{1703}{1728} - \frac{23\pi^2}{72} + \frac{\pi^2}{3} \ln(2) - \frac{173}{288} \zeta(3) + \frac{5}{2} \zeta(5) + \mathcal{O}\left(\frac{m_e}{\bar{q}^2} \ln^2\left(\frac{\bar{q}^2}{m_e^2}\right)\right). \quad (14)$$

The numerical value of the non-logarithmic coefficient is 0.012290603... We have verified the asymptotic expansion (14).

Finally, the three-loop vacuum-polarization correction to the Coulomb potential can be expressed as a generalization of Eq. (63) of Ref. [1],

$$V_R^{(3)}(r) = -\frac{Z\alpha}{\pi} \int_{4m_e^2}^{\infty} \frac{d(q^2)}{q^2} \frac{e^{-qr}}{r} \text{Im}\left[\Pi_R^{(3)}(q^2 + i\epsilon)\right], \quad (15)$$

where according to Eq. (3),

$$\text{Im}\left[\Pi_R^{(3)}(q^2 + i\epsilon)\right] = \left(\frac{\alpha}{\pi}\right)^3 \text{Im}\left[P_R^{(3)}(q^2 + i\epsilon)\right], \quad (16)$$

and $\text{Im}\left[P_R^{(3)}(q^2)\right]$ is given in Eq. (8).

III. NUMERICAL CALCULATION

The energy shift

$$E_{n\ell}^{(3)} = \langle n\ell | V_R^{(3)}(r) | n\ell \rangle = -\frac{Z\alpha}{\pi} \times \int_{4m_e^2}^{\infty} \frac{d(q^2)}{q^2} \left\langle n\ell m \left| \frac{e^{-qr}}{r} \right| n\ell n \right\rangle \text{Im}\left[\Pi_R^{(3)}(q^2 + i\epsilon)\right], \quad (17)$$

can be evaluated in first-order perturbation theory, for a nonrelativistic state with principal quantum number n and orbital angular momentum quantum number ℓ . The energy shift is independent of the magnetic projection m . In writing Eq. (17), we follow the conventions of Refs. [1, 8] for the sign of the vacuum-polarization function. When comparing to the (opposite) sign conventions used in Ref. [18], one notices that in Eq. (10.241) of Ref. [18], the imaginary part of the vacuum-polarization

function is taken at $q^2 - i\epsilon$, *i.e.*, below the cut, leading to consistency with Eq. (17). We have used the results of Ref. [8] for the three-loop vacuum polarization spectral density $\text{Im}[\Pi_{\text{R}}^{(3)}(q^2 + i\epsilon)] = \rho^{(3)}(q^2)$. Specifically, for q^2 above and close to $(2m_e)^2$, we have used the threshold expansion, which is a series in $v = \beta = \sqrt{1 - \frac{4m_e^2}{q^2}}$, and for large q^2 , we used the ‘‘high-energy’’ expansion, which is a series in m_e^2/q^2 . These expansions are provided in supplementary files accompanying Ref. [8], containing exact results for the first 120 terms in the threshold expansion and the first 50 terms in the high- q^2 expansion. For the point where we switched from use of one series to the other, we chose the point where the two truncated series best match each other, which is near $\bar{q}^2 = 8.56 m_e^2$. At that point they are both equal to $-235.325\,929\,481\dots$, with a difference of a few parts in 10^{13} .

It is convenient to define the (dimensionless) β parameter,

$$\beta = \frac{m_e}{Z\alpha m_r}, \quad (18)$$

which is equal to the product of the generalized Bohr radius $a_0 = 1/(Z\alpha m_r)$ and the electron mass (or, equivalently, in natural units, the inverse of the reduced electron Compton wavelength). For muonic bound systems with nuclear charge numbers $1 \leq Z \leq 6$, the nuclear masses and β parameters are (to six significant figures):

$$m(\text{H}) = 938.272 \text{ MeV}, \quad \beta(\mu\text{H}) = 0.737384, \quad (19a)$$

$$m(\text{D}) = 1875.61 \text{ MeV}, \quad \beta(\mu\text{D}) = 0.700086, \quad (19b)$$

$$m(^3\text{He}) = 2808.39 \text{ MeV}, \quad \beta(\mu^3\text{He}) = 0.343843, \quad (19c)$$

$$m(^4\text{He}) = 3727.38 \text{ MeV}, \quad \beta(\mu^4\text{He}) = 0.340769, \quad (19d)$$

$$m(^6\text{Li}) = 5601.52 \text{ MeV}, \quad \beta(\mu^6\text{Li}) = 0.225084, \quad (19e)$$

$$m(^7\text{Li}) = 6533.83 \text{ MeV}, \quad \beta(\mu^7\text{Li}) = 0.224490, \quad (19f)$$

$$m(^9\text{Be}) = 8392.75 \text{ MeV}, \quad \beta(\mu^9\text{Be}) = 0.167774, \quad (19g)$$

$$m(^{10}\text{Be}) = 9325.50 \text{ MeV}, \quad \beta(\mu^{10}\text{Be}) = 0.167565, \quad (19h)$$

$$m(^{10}\text{B}) = 9324.44 \text{ MeV}, \quad \beta(\mu^{10}\text{B}) = 0.134052, \quad (19i)$$

$$m(^{11}\text{B}) = 10252.5 \text{ MeV}, \quad \beta(\mu^{11}\text{B}) = 0.133916, \quad (19j)$$

$$m(^{12}\text{C}) = 11174.9 \text{ MeV}, \quad \beta(\mu^{12}\text{C}) = 0.111503, \quad (19k)$$

$$m(^{13}\text{C}) = 12109.5 \text{ MeV}, \quad \beta(\mu^{13}\text{C}) = 0.111422. \quad (19l)$$

We have calculated the nuclear masses using the formula

$$m \approx A u - Z m_e + \Delta m, \quad (20)$$

where A is the atomic mass number, u the atomic mass unit, and values for the ‘‘mass excess’’ Δm were taken from the pertinent tables in Ref. [19]. These values are equal to the nuclear masses to the level of precision required, since binding energies are negligible at the level of accuracy required for our studies.

In order to evaluate the energy shift (17), it is advantageous to first calculate the matrix element of the operator $Z\alpha \frac{e^{-qr}}{r}$, which can easily be done analytically.

We list results for states with maximum orbital angular momentum ℓ for given principal quantum number n ,

$$\langle 1S | Z\alpha \frac{e^{-qr}}{r} | 1S \rangle = \frac{4(Z\alpha)^2 m_r}{(2 + (q/m_e)\beta)^2}, \quad (21a)$$

$$\langle 2P | Z\alpha \frac{e^{-qr}}{r} | 2P \rangle = \frac{4(Z\alpha)^2 m_r}{(2 + (q/m_e)\beta)^4}, \quad (21b)$$

$$\langle 3D | Z\alpha \frac{e^{-qr}}{r} | 3D \rangle = \frac{64(Z\alpha)^2 m_r}{9(2 + 3(q/m_e)\beta)^6}, \quad (21c)$$

$$\langle 4F | Z\alpha \frac{e^{-qr}}{r} | 4F \rangle = \frac{16(Z\alpha)^2 m_r}{(2 + 3(q/m_e)\beta)^8}. \quad (21d)$$

The results on the right-hand side involve a common scaling factor $(Z\alpha)^2 m_r$ (the generalized Hartree energy), and a residual dependence on the β parameter, which is of order unity for muonic bound systems of interest, and a function of the dimensionless ratio q/m_e , which, likewise, is of order unity for the integration domain relevant to one-loop, two-loop, and three-loop vacuum polarization. Hence, one can understand why the three-loop vacuum-polarization effect is of order $(\alpha/\pi)^3 (Z\alpha)^2 m_r$ for muonic bound systems, and thus, much less suppressed as compared to electronic bound systems.

Finally, the energy shifts $E_{n\ell}^{(3)}$ of Eq. (17) due to irreducible three-loop vacuum polarization are given in Table I.

The contribution of irreducible three-loop vacuum polarization energy corrections have previously been calculated for several transitions in muonic systems. For muonic hydrogen, we can compare our results to Refs. [9, 10]. The reduced mass in this case is $m_r = m_\mu m_p / (m_\mu + m_p)$, where m_μ is the muon mass, and m_p is the proton mass. From Eqs. (18) and (23) of Ref. [9], one infers the result

$$\begin{aligned} E(2P) - E(2S)|_{\mu\text{H}} &= \left[0.013628(6) \right. \\ &\quad \left. + 0.017419(9) \right] \left(\frac{\alpha}{\pi} \right)^3 (Z\alpha)^2 m_r \Big|_{Z=1} \\ &= 0.0019671(7) \text{ meV}. \quad (22) \end{aligned}$$

We observe excellent agreement with the (numerically more precise) result

$$\begin{aligned} E(2P) - E(2S)|_{\mu\text{H}} &= \left[2.6243(1) \times 10^{-3} \right. \\ &\quad \left. - 6.5673(1) \times 10^{-4} \right] \text{ meV} = 0.0019676(1) \text{ meV} \quad (23) \end{aligned}$$

from Table I. The calculations in Refs. [9, 10] were done both from a direct numerical evaluation of the appropriate Feynman diagrams and from use of a Padé approximate developed in Ref. [17]. More recently, a calculation of the 3S-1S transition in muonic hydrogen gave a result of 0.0246 meV (Ref. [20]) for the irreducible three-loop vacuum polarization contribution, consistent with our more precise result 0.024390 meV. In addition, results have been obtained for the 2S-1S transition in the

muonic ions $\mu^7\text{Li}$, $\mu^9\text{Be}$, and $\mu^{11}\text{B}$ [21]. Our results are consistent with all of these but more precise, in view of the avoidance of the numerical uncertainty inherent to the Padé approximants. The calculations reported in Ref. [21] made use of the Padé approximants [17] for a function related to the irreducible three-loop vacuum polarization function for graphs involving one electron loop only (all but the first two diagrams of Fig. 1. Six specific pieces of information about the vacuum-polarization function along with its general analytical properties were used to construct the approximation. The six items were the first three coefficients of the expansion around $q^2 = 0$, the first two coefficients of the expansion in $1/q^2$ for large negative q^2 , and the threshold behavior near $q^2 = (2m_e)^2$. These six quantities were used to construct Padé $[3/2]$ and $[2/3]$ approximants, which were then used to obtain the vacuum-polarization function and the corresponding energy shifts. The contributions of the first two diagrams of Fig. 1, having two electron loops, were computed separately. Our approach, making use of the first 120 terms in the threshold expansion and the first 50 terms in the large negative q^2 expansion, gives an improved representation of the vacuum polarization scalar function, leads to more precise results, and is straightforward to apply.

IV. CONCLUSIONS

We have investigated the contribution of three-loop irreducible vacuum-polarization diagrams to the bound-state energy levels of muonic bound systems. The evaluation of these corrections constitutes a step forward in the detailed knowledge of the spectrum of these bound systems. The three-loop corrections are of order $\alpha^3(Z\alpha)^2 m_r$. It is instructive to compare their numerical magnitude to another class of recently evaluated corrections, namely, electronic vacuum-polarization corrections to the self energy [20–28]. The latter are of order $\alpha^2(Z\alpha)^4 m_r$, and thus, formally, suppressed by an

additional factor of α in comparison to the three-loop vacuum-polarization corrections calculated here. However, quite surprisingly, the corrections due to three-loop vacuum polarization turn out to be of the same order-of-magnitude as the vacuum-polarization corrections to the self-energy. The observation becomes understandable if one considers that the three-loop corrections are suppressed by one power of π more in the denominator, and a lack of a logarithmic enhancement factor $\ln(Z\alpha)$, and a certain suppression in the numerical coefficients multiplying the terms. The three-loop corrections roughly scale only with the second power of the nuclear charge number, Z^2 , and are thus numerically most important in comparison to other corrections for low nuclear charge numbers. Conversely, the three-loop corrections are numerically suppressed in comparison to other corrections which scale with higher powers of the nuclear charge number Z .

The method of calculation used in this paper makes use of the irreducible three-loop vacuum polarization spectral density, which has recently been obtained analytically [8], and specifically of its expansions near threshold and for high negative q^2 . It is relatively easy to obtain the full vacuum polarization function through use of a subtracted dispersion relation, and to verify its asymptotics given in Eq. (14). Our calculations remove the theoretical uncertainty for the energy levels of muonic bound systems with nuclear charge numbers $1 \leq Z \leq 6$ due to irreducible three-loop vacuum-polarization diagrams. These diagrams constitute, from a field-theoretical point of view, probably the most interesting and challenging subset of the $\alpha^5 m_r$ corrections.

ACKNOWLEDGMENTS

This work was supported by the National Science Foundation through Grants PHY-2308792 (G.S.A.) and PHY-2110294 (U.D.J.), and by the National Institute of Standards and Technology Grant 60NANB23D230 (G.S.A.).

-
- [1] S. Laporta and U. D. Jentschura, *Dimensional regularization and two-loop vacuum polarization operator: Master integrals, analytic results and energy shifts*, Phys. Rev. D **109**, 096020 (2024).
- [2] K. Pachucki, *Theory of the Lamb shift in muonic hydrogen*, Phys. Rev. A **53**, 2092–2100 (1996).
- [3] C. G. Parthey, A. Matveev, J. Alnis, R. Pohl, T. Udem, U. D. Jentschura, N. Kolachevsky, and T. W. Hänsch, *Precision measurement of the hydrogen-deuterium $1S$ – $2S$ isotope shift*, Phys. Rev. Lett. **104**, 233001 (2010).
- [4] U. D. Jentschura, *Lamb shift in muonic hydrogen—I. Verification and update of theoretical predictions*, Ann. Phys. (N.Y.) **326**, 500–515 (2011).
- [5] U. D. Jentschura, *Lamb shift in muonic hydrogen—II. Analysis of the discrepancy of theory and experiment*, Ann. Phys. (N.Y.) **326**, 516–533 (2011).
- [6] M. Baker and K. Johnson, *Quantum electrodynamics at small distances*, Phys. Rev. **183**, 1292–1299 (1969).
- [7] E. de Rafael and J. L. Rosner, *Short-distance behavior of quantum electrodynamics and the Callan–Symanzik equation for the photon propagator*, Ann. Phys. (N.Y.) **82**, 369–406 (1974).
- [8] A. I. Onishchenko, *Three-loop photon spectral density in QED*, e-print arXiv:2212.03502v1 [hep-ph].
- [9] T. Kinoshita and M. Nio, *Sixth-order vacuum-polarization contribution to the Lamb shift of muonic hydrogen*, Phys. Rev. Lett. **82**, 3240–3243 (1999), [Erratum Phys. Rev. Lett. **103**, 079901 (2009)].
- [10] T. Kinoshita and M. Nio, *Accuracy of calculations involving α^3 vacuum-polarization diagrams: Muonic hydrogen*

- Lamb shift and muon $g - 2$* , Phys. Rev. D **60**, 053008 (1999).
- [11] V. G. Ivanov, E. Yu. Korzinin, and S. G. Karshenboim, *Second-order corrections to the wave function at the origin in muonic hydrogen and ponium*, Phys. Rev. D **80**, 027702 (2009).
- [12] J. Schwinger, *Particles, Sources and Fields (Volume III)* (Addison-Wesley, Reading, MA, 1973).
- [13] R. E. Cutkosky, *Singularities and discontinuities of Feynman amplitudes*, J. Math. Phys. **1**, 429–433 (1960).
- [14] R. N. Faustov, A. L. Kataev, S. A. Larin, and V. V. Starshenko, *The analytical contribution of the three-loop diagrams with two fermion circles to the photon propagator and to the eighth-order correction to the muon anomalous magnetic moment*, Phys. Lett. B **254**, 241–246 (1991).
- [15] A. L. Kataev, *Renormalization group and the five-loop QED asymptotic contributions to the muon anomaly*, Phys. Lett. B **284**, 401–409 (1991).
- [16] D. J. Broadhurst, A. L. Kataev, and O. V. Tarasov, *Analytical on-shell QED results: 3-loop vacuum polarization, 4-loop β -function and the muon anomaly*, Phys. Lett. B **298**, 445–452 (1993).
- [17] P. A. Baikov and D. J. Broadhurst, *Three-loop QED vacuum polarization and the four-loop muon anomalous magnetic moment*, in *New Computing Techniques in Physics Research IV*, ed. by B. Denby and D. Perret-Gallix (World Scientific, Singapore, 1995), and e-print arXiv:hep-ph/9504398.
- [18] U. D. Jentschura and G. S. Adkins, *Quantum Electrodynamics: Atoms, Lasers and Gravity* (World Scientific, Singapore, 2022).
- [19] F. G. Kondev, M. Wang, W. J. Huang, S. Naimi, and G. Audi, *The NUBASE2020 evaluation of nuclear physics properties*, Chin. Phys. C **45**, 030001 (2021).
- [20] A. E. Dorokhov, R. N. Faustov, A. P. Martynenko, and F. A. Martynenko, *Energy interval $3S-1S$ in muonic hydrogen*, Phys. Rev. A **102**, 062820 (2020).
- [21] A. E. Dorokhov, R. N. Faustov, A. P. Martynenko, and F. A. Martynenko, *Precision physics of muonic ions of lithium, beryllium and boron*, Int. J. Mod. Phys. A **36**, 2150022 (2021).
- [22] B. J. Wundt and U. D. Jentschura, *Semi-analytic approach to higher-order corrections in simple muonic bound systems: Vacuum polarization, self-energy and radiative-recoil*, Eur. Phys. J. D **65**, 357–366 (2011).
- [23] E. Borie, *Lamb shift in light muonic atoms—Revisited*, Ann. Phys. (N.Y.) **327**, 733–763 (2012).
- [24] E. Yu. Korzinin, V. G. Ivanov, and S. G. Karshenboim, *$\alpha^2(Z\alpha)^4m$ contributions to the Lamb shift and the fine structure in light muonic atoms*, Phys. Rev. D **88**, 125019 (2013).
- [25] A. A. Krutov, A. P. Martynenko, G. A. Martynenko, and R. N. Faustov, *Theory of the Lamb shift in muonic helium ions*, JETP **120**, 73–90 (2015).
- [26] A. E. Dorokhov, A. P. Martynenko, F. A. Martynenko, O. S. Sukhorukova, and R. N. Faustov, *Energy interval $1S-2S$ in muonic hydrogen and helium*, JETP **129**, 956–972 (2019).
- [27] K. Pachucki, V. Lensky, F. Hagelstein, S. S. Li Muli, S. Bacca, and R. Pohl, *Comprehensive theory of the Lamb shift in light muonic atoms*, Rev. Mod. Phys. **96**, 015001 (2024).
- [28] B. Ohayon and U. D. Jentschura, *Reexamination of vacuum-polarization corrections to the self-energy in muonic bound systems*, Phys. Rev. A **110**, 032820 (2024).